Journal Pre-proofs

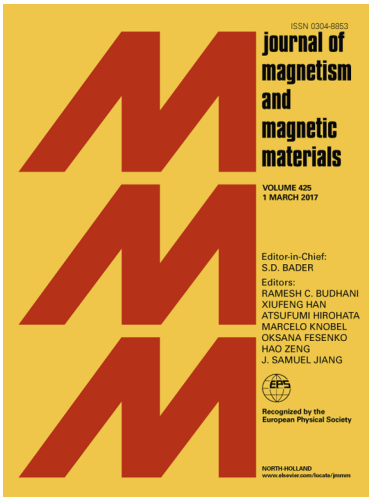

Asymmetric ascending and descending loop shift exchange bias in $Bi_2Fe_4O_9$-$BiFeO_3$ nanocomposites

Tuhin Maity, Saibal Roy

PII: S0304-8853(19)31196-5
DOI: https://doi.org/10.1016/j.jmmm.2019.165783
Reference: MAGMA 165783

To appear in: *Journal of Magnetism and Magnetic Materials*

Received Date: 2 April 2019
Revised Date: 2 September 2019
Accepted Date: 2 September 2019

Please cite this article as: T. Maity, S. Roy, Asymmetric ascending and descending loop shift exchange bias in $Bi_2Fe_4O_9$-$BiFeO_3$ nanocomposites, *Journal of Magnetism and Magnetic Materials* (2019), doi: https://doi.org/10.1016/j.jmmm.2019.165783

Asymmetric ascending and descending loop shift exchange bias in $Bi_2Fe_4O_9$-$BiFeO_3$ nanocomposites

Tuhin Maity[1,2,*] and Saibal Roy[1,3,*]

[1]*Micropower-Nanomagnetics Group, Micro-nano-systems Center, Tyndall National Institute, University College Cork, Lee Maltings, Dyke Parade,* Cork, Ireland

[2] *Department of Materials Science and Metallurgy, University of Cambridge, Cambridge, CB3 0FS, United Kingdom*

[3]*Department of Physics, University College Cork (UCC), Cork, Ireland*

Corresponding authors: tsm38@cam.ac.uk ; saibal.roy@tyndall.ie

Abstract: We show detail study of asymmetric exchange bias originating from asymmetric behaviour of ascending and descending loops of the magnetic hysteresis of $Bi_2Fe_4O_9$ - $BiFeO_3$ multiferroics nanocomposites. Detail magnetometry study reveals the co-existence of super spin glass (SSG) and dilute antiferromagnet in a field (DAFF) at the interface between antiferromagnetic (AFM) $BiFeO_3$ and ferromagnetic (FM) $Bi_2Fe_4O_9$ in nanocomposite particles. The interfacial spins behave differently for positive and negative fields and result into asymmetric exchange bias, which has been precisely identified by several critical magnetic measurements such as training effect, stop & wait protocol, isothermal remanence (IRM) & thermoremanence (TRM) measurements, and high field relaxation measurement. The DAFF spins, which generate non-switchable unidirectional anisotropy at the complex FM-SSG-DAFF-AFM interface below Vogel-Fulcher freezing temperature of $BiFeO_3$ at 29.4 K, are solely responsible for such asymmetry in exchange bias.

Keywords: Exchange bias, multiferroics, spin glass, nanocomposites

1. Introduction:

Exchange bias (EB) is one of the most studied phenomenon in magnetism due to its critical role in developing fundamental understanding and various spintronic device applications. Even after 70 years of its discovery the exchange bias phenomenon is not well understood due to its complexity, and exciting new phenomena are being observed in different types of materials till date. [1-4] As the electronic devices are miniaturized continuously, the use of nanoparticle (NP) embedded systems is gaining interest in research community gradually. Chemically synthesised bi-magnetic NPs show interesting phenomenon due to its complex interfacial spin structure. [5-8] Several nanoparticle systems show unconventional exchange bias phenomenon such as asymmetric exchange bias due to complex interfacial spins and their interactions. [9-11] The basic signature of exchange bias is manifested in the magnetic hysteresis loop which is normally a symmetric reversal process, where magnetization reverses non-linearly from one saturation state to the opposite saturation state during field reversal. Due to the existence of EB the hysteresis loop shifts along field axis where the direction of shift depends on the bias field and/or loop tracing protocol. Since the hysteresis loop is a symmetric reversal process, it is expected that the loop shift should be equal for both ascending and descending loops. However, often it is observed that such overall hysteresis

loop shift originates due to major shift in one loop (such as ascending loop) where the other loop (such as descending loop) experiences minor shift. [12-18] This resulted into asymmetric EB phenomenon in different systems. Additionally, such asymmetry in ascending and descending loop shift is often observed during magnetic training with reduction of EB due to spin reorientation, ideally, which should be symmetric in the field reversal process. In this report we have observed such asymmetric EB which originates due to asymmetric shift in ascending and descending parts of the hysteresis loops in $Bi_2Fe_4O_9$ - $BiFeO_3$ (BFO) multiferroic nanocomposite. The asymmetric EB depends on the both bias field and hysteresis loop tracing protocol. This has been investigated by different magnetic experiments namely training effect, stop & wait protocol, isothermal remanence (IRM), thermoremanence (TRM) and high field demagnetization measurements. From these tailored high-resolution measurements it is identified that the DAFF at the interface freezes and become responsible for the asymmetry in the ascending loop part of the magnetic hysteresis.

2. Experimental procedure:

The BFO nanocomposite was synthesized by sonochemical route. [19] Composite nanoparticles of two different sizes (A and B) were prepared. The nanoparticles were found to contain ~90 (A) & 94 (B) vol% antiferromagnetic (AFM) $BiFeO_3$ and ~10 & 6 vol% ferromagnetic (FM) $Bi_2Fe_4O_9$ respectively. The volume fraction of the two phases were determined by x-ray diffraction and consequent Rietveld refinement analysis. The average sizes were identified as ~57 nm (A) & 112 nm (B) for $BiFeO_3$ and ~13 nm (A) & 19 nm (B) for $Bi_2Fe_4O_9$ parts. The particles had an apparent size distribution and did not agglomerate as observed by high-resolution transmission electron microscopy (HRTEM). The detail structural characterizations were done by HRTEM and selected area electron diffraction (SAED) method respectively. [10, 15] The HRTEM images are shown in Fig. 1. The magnetic properties were investigated in a superconducting quantum interference device (SQUID) magnetometer (MPMS XL 5, Quantum Design) across a temperature range of 2–350 K and under a maximum applied field of 50 kOe. The canted AFM $BiFeO_3$ requires very high field to saturate. However, small FM $Bi_2Fe_4O_9$ particles can be saturated way below 50 kOe field. [20] Prior to each measurement the samples were demagnetized at 350K (much above the T_B) by heating up the sample space, following an appropriate protocol, where an applied high field was reduced to zero by oscillating field with varying amplitude (positive/negative) e.g. (+1000) → (-800) → (+600) → (-400).....(+5) → (-4) → (+3) → (-2) → (+1) → (0). Both the nanocomposite particle systems show asymmetric spontaneous (SEB) and conventional (CEB) exchange bias. The average size of the FM $Bi_2Fe_4O_9$ part is smaller than single domain size and behave as superparamagnetic. The A nanocomposite with average $Bi_2Fe_4O_9$ size 13 nm shows blocking temperature (T_B) at ~60 K and above T_B the magnetization completely disappears. The T_B of 'B' nanocomposite is higher than 350 K since the average diameter of $Bi_2Fe_4O_9$ is higher (19 nm) compared to A nanocomposite and T_B is proportional to the volume. Hence, it is difficult to remove any asymmetry from 'B' sample within the SQUID temperature limit of 350K. Therefore, we particularly chose 'A' nanocomposite sample for further investigation due to the low T_B above which the sample can be completely demagnetized and magnetic anisotropy can be destroyed.

3. Experimental results:

3.1. Asymmetric exchange bias

In Fig. 2, the conventional exchange bias (CEB) measurements for different conditions have been shown. The sample was cooled down from 350 K (way above the T_B of B particles) to 2K under ±50kOe cooling field. Then hysteresis loops were measured for two different loop tracing protocols: : +50 kOe → 0 → −50 kOe → 0 → +50 kOe (positive or P loop) or −50 kOe → 0 → +50 kOe → 0 → −50 kOe (negative or N loop). Four types of exchange bias (H_E) were measured: a. positive field cooled and positive loop tracing i.e. $+H_{EP}$, b. negative field cooled and negative loop tracing i.e. $-H_{EN}$, c. Positive field cooled with negative loop tracing i.e. $+H_{EN,}$ and d. Negative field cooled with positive loop tracing i.e. $-H_{EP}$. Four different EB and related descending loop coercivity (H_{C1}) and ascending loop coercivity (H_{C2}) are listed in the Table 1 for comparison and shown in Fig.2.

Table 1. Different coercive parameters and exchange bias for different exchange bias loop tracing.

		Field Cool	**Hysteresis**	**H_{C1} (Oe)**	**H_{C2} (Oe)**	**H_C (Oe)**	**H_E (Oe)**
a	$+H_{EP}$	+50 kOe	Positive	-2900	-300	1300	-1600
b	$-H_{EN}$	-50 kOe	Negative	600	3050	1225	1825
c	$+H_{EN}$	+50 kOe	Negative	-2400	-600	900	-1500
d	$-H_{EP}$	-50 kOe	Positive	900	2400	750	1650

Further, training effect measurements were carried out to probe the dynamics of the spin structure at the interfaces for both positive and negative bias field. The dependence of H_E on the number of repeating cycles (n) is shown in Fig. 3.a. The H_E obtained under a bias field of both positive and negative 50 kOe field is shown here. It is clearly observed that the training effect is more prominent for the negative bias field compared to the positive bias field. The corresponding coercive fields for ascending and descending curve is plotted in Fig. 3 (b) and (c) for positive and negative training respectively.

3.2. Spin relaxation under low and high-field

To understand the exact origin of such interesting asymmetric phenomenon we did different complex magnetic measurements assigned to delineate different magnetic spin components and their interactions. Previously we reported that in such BFO nanocomposites SSG and DAFF spin structure coexist. [15] We have studied the high field relaxation of the magnetization at 2 K over a time span of 6000 s with ±50 kOe field to investigate the effect of SSG. The sample was demagnetized at 350 K and then cooled down to 2 K under zero field. After that a field of +50 kOe was applied and the moment (M) was measured for 6000s. Following that, the field was switched to −50 kOe and then to +50 kOe. The magnetization was measured for 6000s under each condition. The absolute change of magnetization (|M|) for these three high fields switching as a function of time is plotted in Fig. 4 which is found to be typical of relaxation behaviour of SSG.

Further, well designed stop & wait protocols or memory effect measurements were done to probe the SSG at the interface and its effect on asymmetric loop shift (Fig. 5.a). [10] The sample was first cooled down to 2 K from room temperature without any applied field and then moment vs temperature (MT) was measured while heating it up with +20 Oe bias field. Similar measurement was done again. However, the zero field cooling (ZFC) was stopped at a random temperature below T_B: 20K for 10^4 sec. The difference in MT measurement with respect to the first measurement, δM, is plotted (the black curve of the inset figure in Fig. 5.a) which shows a dip at the stopping temperature of 20K while cooling. Such effect is called memory effect and a typical signature of SSG. Similar measurement was done for -20 Oe bias field (the red curve of the inset figure in Fig. 5.a). Relative change in magnetization for opposite field is plotted together and they seem to coincide with each other.

Another magnetic component contributing to overall magnetic behaviour is the main ferromagnetic part, $Bi_2Fe_4O_9$. To investigate its contribution towards the asymmetric reversal we did high field demagnetization measurement for the reversal of FM $Bi_2Fe_4O_9$. For this measurement, first a large positive field (+50kOe) was applied. Subsequently a small negative field is applied, then removed and remanence magnetization is measured (Blue curve Fig. 5.b). The non-zero value at -50 kOe is due to the existence of SSG and exchange coupling at the interface. Similar measurement was done for negative field (Red curve Fig. 5.b). Both positive and negative demagnetization shows similar behaviour. From both high field relaxation, memory effect and high field demagnetization measurement it is clear that the asymmetry does not originate from SSG at the interface or FM $Bi_2Fe_4O_9$.

3.3. Asymmetric behaviour of DAFF

Third magnetic component in the BFO nanocomposite is DAFF spins. To investigate the DAFF spins we further carried out isothermal remanence (IRM) and thermoremanence (TRM) measurements at 2 K for both positive and negative field directions. For the TRM measurement, the sample was cooled down from 350K to 2 K under a defined field. Then the field was removed and the remanent magnetization was measured immediately. For the IRM measurement the sample was cooled down to 2K from 350 K under zero field. Momentarily a defined field was applied and removed. Immediately the remanent magnetization was measured. These measurements were done for both positive and negative fields. The field dependence of the TRM & IRM at 2 K is shown in Fig. 6. (a & b).

4. Discussion:

The maximum exchange bias for both positive and negative loops were observed when the sample was cooled down with positive field (+) and measured with positive starting field and vice versa (Fig. 2). The amount of exchange bias is higher for negative field cooled measurement with negative loop tracing i.e. $-H_{EN}$~1825 Oe compared to the positive field cooled measurement with positive loop tracing i.e. $+H_{EP}$~1600 Oe. Further, the exchange bias was measured where cooling field and the starting field of hysteresis loops tracing are opposite i.e. + H_{EN} and -H_{EP}. The exchange bias was decreased by 100 Oe for positive field cooled and 200 Oe for negative field cooled measurement. Since an ideal hysteresis loop is a symmetric reversal process this 100 Oe (or 200 Oe) loop shift should originate from equal amount of shift i.e. 100 Oe (or 200 Oe) in both descending and ascending loops. However, it

is observed that the descending loop shift of -500 Oe is much higher than the ascending loop shift of -200 Oe. Similar behaviour was observed for negative bias field but in opposite direction. It is clearly observed that the magnitude of the exchange bias does not change much due to change of cooling field for positive loop tracing ($|\Delta H_{EP}|$=50 Oe) compared to much higher change ($|\Delta H_{EP}|$=325 Oe) for negative loop tracing which is conspicuous.

The training effect measurement in Fig. 3.a clearly shows that the effect is much stronger for negative field. In Fig. 3.b & c the individual training in descending and ascending loops is plotted. In both the training effect measurements it is clearly observed that the shift in ascending curve dominates the training effect. Hence, it is assumed that unless there is a frozen unidirectional anisotropy at the exchange bias interface such asymmetry could not be observed. A significant drop in H_{C2} between n = 1 and n = 3 for both positive and negative field is observed whereas H_{C1} seen to be slowly changing even up to 5th cycle. Hence the training effect becomes insignificant for H_{C2} when n≥3 but not for H_{C1}. Hence, it is understood that the EB arises from two spins namely, one is weekly-coupled spin and the other is strongly coupled spin at the interface.

In the high field relaxation measurements all three plots clearly show an upward creep due to the incoherent rotation of the super spin glass (SSG) at the interface (Fig. 5.a). The three curves are individually fitted with single spin relaxation equation $M = M_0 + A*exp\ (R_0*t)$ and the equation fits very well. The fitting parameters (M_0, A and R_0) are included in the respective plots. Further we fitted the curve with double spin model. However, the fitting does not improve significantly. This confirms that the rotation of SSG for field reversal is coherent and symmetric. To confirm this further we did well designed stop & wait protocol or memory effect measurements for positive and negative bias field. Exactly opposite result was observed (red curve in the inset Fig. 5.a). Both the normalised δM is plotted together for positive and negative bias field and they exactly coincide with each other. Hence it is proved that the relaxation of SSG even for low opposite fields is symmetric. Since SSG follows a symmetric reversal then it should be strongly coupled spin as observed in training effect. Further, the high field demagnetization shows symmetric reversal for both positive and negative field. As the moment was immediately measured after removing the field during the process the spin-glass will not have any effect in this measurement. Rather a non-zero remanence magnetization was observed at the ±50 kOe reverse field which is due to aligned SSG or exchange coupled spins. Hence, the reversal of FM $Bi_2Fe_4O_9$ which is the main contributor to overall magnetization is symmetric.

The IRM and TRM are unique measurement protocols to understand the DAFF spins. In IRM & TRM plots we observed that the IRM exhibits a weak field dependence, and the TRM shows $\propto H^{\nu H}$ pattern. Such behaviour is found in two-dimensional DAFF spin structure. [21] The TRM behaviour for both positive and negative fields are similar which is confirmed by the fitting where νH is 0.57 and 0.64 for positive and negative fields respectively. [22] Interestingly the IRM behaviour for positive and negative fields is very different. The IRM curve exponentially decay with the field. For negative field the effect in IRM is much stronger where the decay constant is 2.34 compared to 1.67 for positive field as obtained from the curve fitting. Since TRM is a thermal process the anisotropy created by DAFF along the field cooled direction is symmetric for both positive and negative field as the system is cooled down from room temperature which is way above blocking temperature and Vogel-Fulcher freezing temperature of $BiFeO_3$ at 29.4 K. [23] In IRM the system is cooled down

through the T_B and Vogel-Fulcher freezing temperature without any field. Hence an irreversible spontaneous anisotropy is created by the DAFF spins at the interface. This spontaneous anisotropy is negative in nature as observed in the field independent cooling of the sample in IRM measurement.

To investigate such irreversibility of DAFF interface and its effect in the anisotropic EB behaviour we investigated field dependent M vs T. The zero field cooling (ZFC) and field cooling (FC) magnetization measurements were performed with different applied fields. For ZFC measurements, first the sample was cooled from 100 to 2 K in zero magnetic field. Then at 2 K a magnetic field was applied and the magnetic moment was recorded during warming (ZFC) and again during cooling (FC) (Fig. 7.a). In the ZFC-FC curve the point of bifurcation between FC and ZFC and the irreversibility of the ZFC determine the T_B and the irreversibility temperature (T_{irr}). It is observed that the T_B initially decrease with the field and then stop changing. But the T_{irr} keep decreasing with the applied field (Fig. 7.b). For Ising spin systems, de Almeida and Thouless have predicted the dependence of T_{irr} on H: $\frac{H}{\Delta J}\alpha \left(1-\frac{T_{irr}}{T_F}\right)^{3/2}$, where T_F is the zero-field SG freezing temperature and ΔJ the width of the distribution of exchange interactions. [22] Fig. 7.c shows the $H^{2/3}$ dependency of T_{irr} which is nearly linear. The extrapolated linear fit to H = 0 gives the zero-field SG transition (T_F) at 27 K which is close to the Vogel-Fulcher freezing temperature at 29.4 K for $BiFeO_3$. [23] The extrapolation of the linear fit back to H= 0 allows to estimate the critical field above which uniaxial anisotropy of DAFF vanishes, which appears to be about 1185 Oe, very close to the difference between the maximum descending and ascending coercive field i.e. 1150 Oe. Hence the frozen anisotropy created by the DAFF spins while cooling is solely responsible for the ascending field dominated asymmetry in the observed exchange bias. Such frozen anisotropy can also be generated from the presence of the long-range Ising spin glasses due to the possible absence of Fe ions in interfacial defect layer, which could potentially work as a nonmagnetic spacer between magnetic layers. The free energy for such multi spin system can be expressed as:

$$E = -\mu_0 H\sum_i M_i t_i \cos(\theta-\theta_i) + \sum_i k_i t_i sin^2\theta_i - J_E\sum_{i\neq i} S_i S_i \cos\theta_i \text{ ---------- 1}$$

where, H is the external magnetic field at an angle θ with respect to the external magnetic field, M_i is saturation magnetization of different (i) spins, t_i is the thicknesses for the respective layer, and k_i is the anisotropy constants of the respective layer, θ_i is the angles between the external magnetic field and the moments of respective spin, and J_E defines the exchange coupling strength between the spins at the interface. For the strictly monotonic decrease or increase as observed by high field relaxation and training effect measurements, the equilibrium magnetization can be written as: $S_i = \lim_{n\to\infty} S_i(n)$, where n= number of configurations. [24] The microscopic change in magnetization is $\delta S_n = S_i(n) - S_i$. Such change in interfacial magnetization would also change the free energy from positive to negative i.e. $\Delta|E(\delta S_n) = \Delta E(-\delta S_n)$. This free energy is equivalent to the demagnetization energy, which is required to stabilise the system. Considering higher order stabilization has insignificant contribution, the relaxation of the system can be determined by the Landau-Khalatnikov (LK) equation [25]:

$$\xi \dot{S_i} = -\frac{\partial \Delta E}{\partial S_i} \text{ ---------- } 2$$

where ξ is a phenomenological damping constant and $\dot{S_i}$ is time derivative of S_i. As observed by above described different magnetic measurements the relaxation process of interfacial spins is very slow with respect to the microscopic spin fluctuations. Hence, left hand side of the equation 2 cannot be zero. Thus, any frozen spin at the interface will have a discretized effect on the energy reversal process. For any possible maxima and minima condition where $\theta = \pm\theta_i$, any frozen spin in the system will result into $\frac{\partial E}{\partial \theta_i} \neq 0$. Due to the existence of DAFF spins at the interface which creates a frozen unidirectional anisotropy in negative direction for negative exchange bias, the ascending field dominated asymmetry in exchange bias is observed in this $Bi_2Fe_4O_9$ - $BiFeO_3$ multiferroics nanocomposite system. Why such negative anisotropy originates is unknown yet. Therefore, it seems purposeful to devote a theoretical study to understand this complex multi-layer exchange bias system along with Neutron diffraction study, which will be pursued in future.

5. Conclusion:

In this report, we have thoroughly investigated the asymmetric loop shift of ascending and descending curve of the exchange coupled BFO nano-composite. Different critical magnetic measurements show the existence of four different magnetic components namely ferromagnetic core, antiferromagnetic shell, super spin glass (SSG) and dilute antiferromagnet in a field (DAFF) spins at the interface. Detail magnetometry reveals the origin of such asymmetric exchange bias is from the DAAF spins. A unidirectional frozen spontaneous anisotropy is generated by DAFF in the exchange interactions between FM and AMF part via SSG & DAFF, which give rise to asymmetric giant EB. This study will help to understand several similar exchange bias, nano composite and multiferroic systems and pave the way for their potential application in miniaturized electronic devices.

Acknowledgement:

The work is financially supported by Horizon 2020 ASCENT EU project (Access to European Nanoelectronics Network -Project no. 654384). TM acknowledges funding from the Irish Research Council Project (No. GOIPD/2016/474). The authors acknowledge Dipten Bhattacharya (CGCRI-India) for providing the samples.

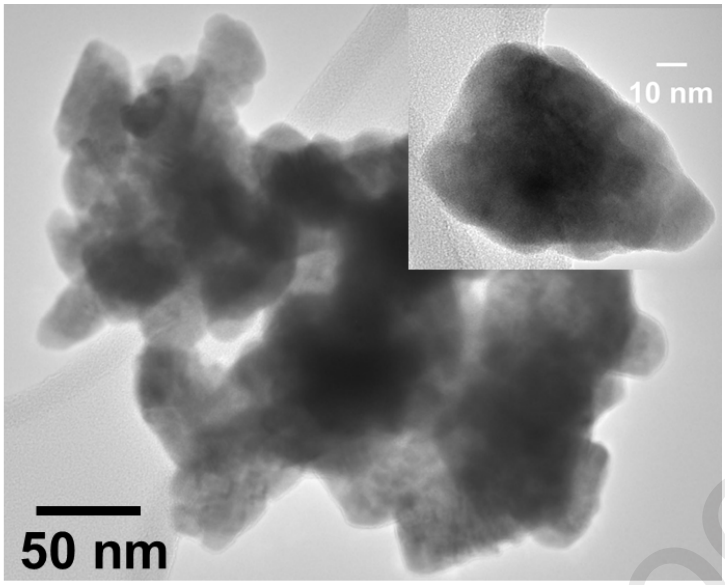

Figure 1. HRTEM image of BFO nanocomposite. The average particle size was ~57nm.

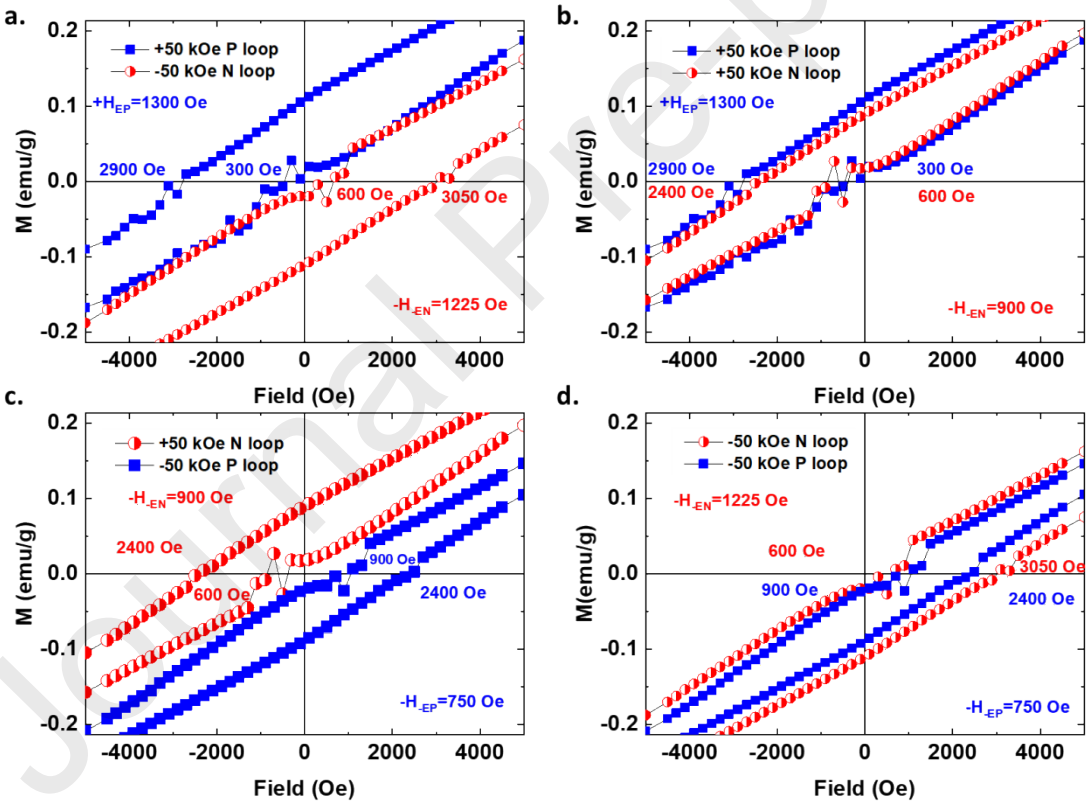

Figure 2. Exchange bias was measured for both positive and negative bias field followed by both positive and negative loop tracing protocols. All exchange bias combinations are shown for comparison.

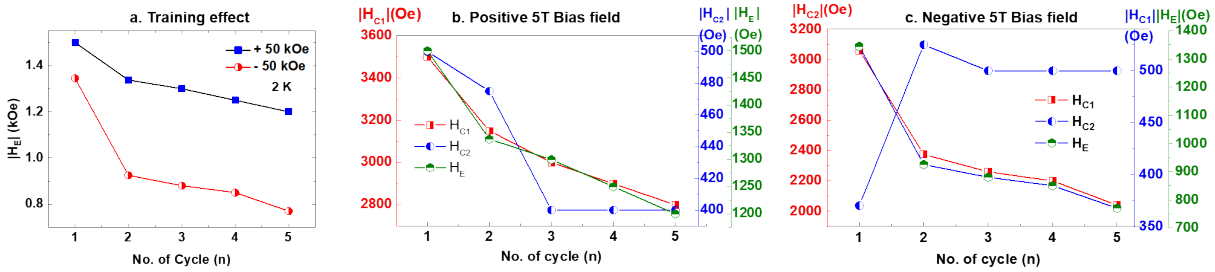

Figure 3. (a) The training effect was done for 5 cycles for both positive and negative bias fields. (b & c) The individual training in ascending and descending loops for both positive and negative field are shown respectively.

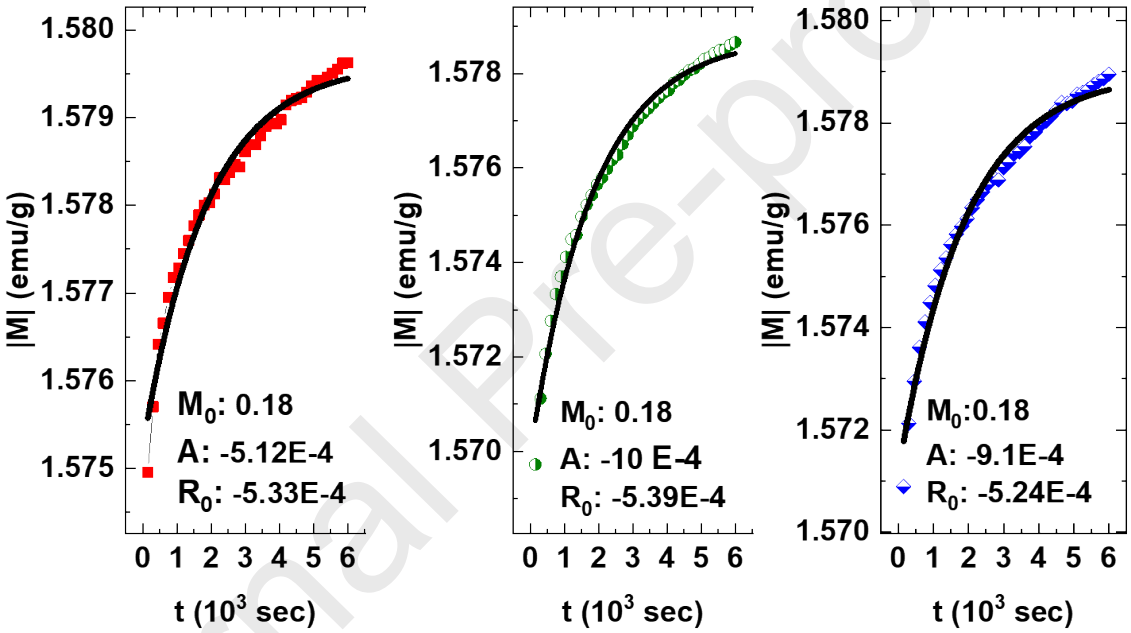

Figure 4. High field relaxation measurement was done for positive +50 kOe and -50 kOe which shows symmetric switch of the magnetization for positive and negative fields. The fitting parameters are M_0, A and R_0 (up → down)

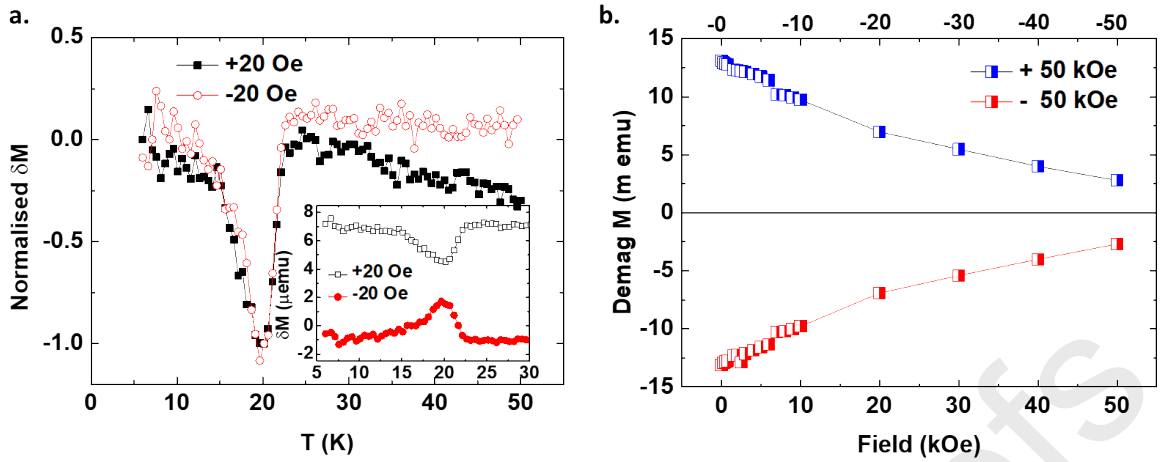

Figure 5. (a) Stop & wait protocol for positive and negative bias field was done. The observed memory effect for opposite fields is symmetric. (b) High field positive and negative demagnetization shows symmetric reversal of magnetization.

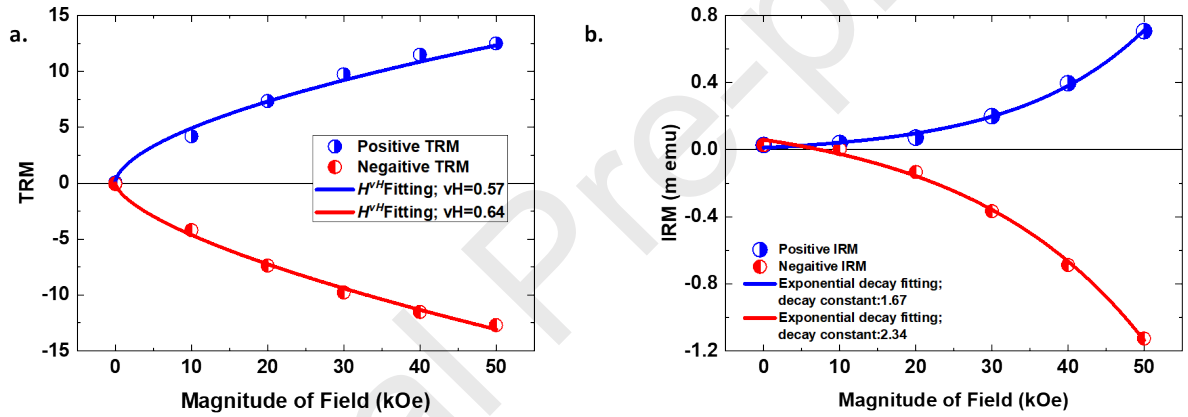

Figure 6. TRM and IRM measurements for both positive and negative. Asymmetric behaviour was observed in IRM measurement but not in TRM measurement. This confirm the asymmetric behaviour of 2D-DAFF.

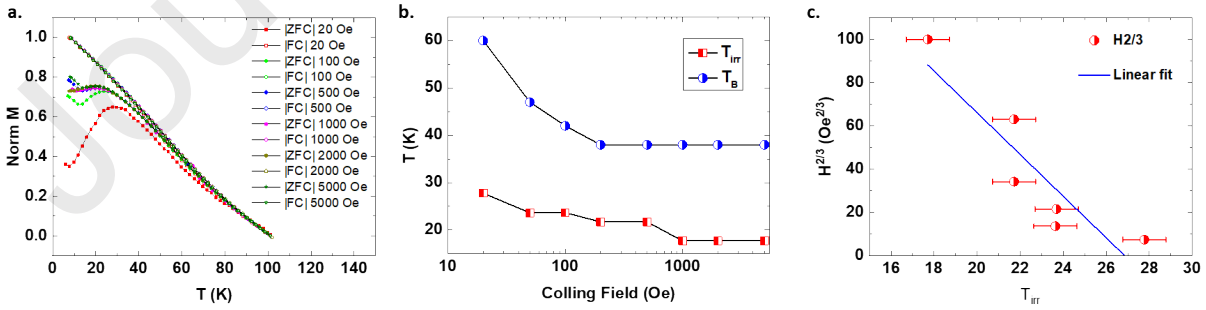

Figure 7. (a) MT measurement was done for different bias field. (b) The blocking temperature (T_B) initially decreases with the field and then stops. The irreversible temperature T_{irr} decreases with increase of field. (c) The T_{irr} shows linear dependency on $H^{2/3}$. The error bar refers to possible measurement error in temperature.

Reference:

1. W. H. Meiklejohn and C. P. Bean; Phys. Rev. 105, 904 (1957)
2. J. Nogues & I.K. Schuller; J. Magn. Magn. Mater. 192, 203-232 (1999)
3. A.E. Berkowitz, K. Takano; J. Magn. Magn. Mater. 200, 552-570 (1999)
4. M. Kiwi; J. Magn. Magn. Mater. 234, 584–595 (2001)
5. T. Maity, S. Roy; J. Magn. Magn. Mater. 465, 100–105F(2018)
6. V. Skumryev, S. Stoyanov, Y. Zhang, G. Hadjipanayis, D. Givord, J. Nogués, Nature 423, 850–85 (2003)
7. K. Simeonidis, C. Martinez-Boubeta, O. Iglesias, A. Cabot, M. Angelakeris,S. Mourdikoudis, I. Tsiaoussis, A. Delimitis, C. Dendrinou-Samara, O. Kalogirou, Phys. Rev. B 84 , 144433, (2011)
8. H. Khurshid, W.F. Li, M.H. Phan, P. Mukherjee, G.C. Hadjipanayis, H. Srikanth, Appl. Phys. Lett. 101 (2) 022403, (2012)
9. J. Camarero, J. Sort, A. Hoffmann, J. M. Garcia-Martin, B. Dieny, R. Miranda, and J. Nogues; Phys. Rev. Lett. 95, 057204 (2005)
10. T. Maity, S. Goswami, D. Bhattacharya, S. Roy; Phys. Rev. Lett. 110 (10), 107201(2013), 114 (9), 099704 (2015)
11. M. Hudl, R. Mathieu and P. Nordblad; Scientific Reports, 6, 19964 (2016)
12. R. Wen-Bin, H. Mao-Cheng, Y. Biao, S. Zhong, Z. Shi-Ming, X. Ming-Wen, G. Yuan, Z. Wei, S. Li and D. Jun; Chin. Phys. B 23, 10 107502 (2014)
13. G. Salazar-Alvarez, J. Sort, S. Surinach, M. Dolors Baro, and J. Nogues; J. Am. Chem. Soc., 129, 9102-9108 (2007)
14. T. Maity, S. Goswami, D. Bhattacharya, G. C. Das, S. Roy; J. Appl. Phys. 113 (17), 17D916 (2013)
15. T. Maity, S. Goswami, D. Bhattacharya, S. Roy; Phys. Rev. B 89 (14), 140411 (2014)
16. R. Wu et al J. Phys. D: Appl. Phys. 48 275002 (2015)
17. J. Barzola-Quiquia, A. Lessig, A. Ballestar, C. Zandalazini, G. Bridoux, F. Bern and P. Esquinazi; J. Phys.: Condens. Matter 24, 366006 (2012)
18. X. Yuan , X. Xue , J. Du, F. Z. Huang, Q. Xu; Solid State Communications 161, 9–12 (2013)
19. S. Goswami, D. Bhattacharya, and P. Choudhury; J. Appl. Phys. 109, 07D737 (2011)
20. L. Wu, C. Dong, H. Chen, J, Yao, C, Jiang, D. Xue; J. Am. Ceram. Soc.,95 (12) 3922–3927 (2012)
21. M. J. Benitez, O. Petracic, E. L. Salabas, F. Radu, H. Tuysuz, F. Schuth, and H. Zabel, Phys. Rev. Lett. 101, 097206 (2008)
22. J. L. Tholence and R. Tournier, J. Phys. (Paris) Colloq. 35, C4-229 (1974)
23. Manoj K. Singh, W. Prellier, M. P. Singh, Ram S. Katiyar, and J. F. Scott, Phys. Rev. B 77, 144403 (2008)
24. J. R. L. de Almeida and D. J. J. Thouless. Phys. A: Math. Gen. 11 983 (1978)
25. L. D. Landau and I. M. Khalatnikov, Dokl. Akad. Nauk SSSR 96, 469 (1954)